

## Facile and Catalytic Synthesis of Conductive Titanium Suboxides for Enhanced Oxygen Reduction Activity and Stability in Proton Exchange Membrane Fuel Cells

Young-Woo Lee<sup>1</sup>, Da-Hee Kwak<sup>1</sup>, Ah-Reum Park<sup>1</sup>, Bumwook Roh<sup>2</sup>, Inchul Hwang<sup>2</sup>, Guozhong Cao<sup>3</sup>, Kyung-Won Park<sup>1,\*</sup>

<sup>1</sup> Department of Chemical Engineering, Soongsil University, Seoul 156-743, Republic of Korea

<sup>2</sup> Hyundai Motor Company, Mabuk-Ri, Gyeonggi-Do 446-912, Republic of Korea

<sup>3</sup> Department of Materials Science and Engineering, University of Washington, Seattle, WA 98195, USA

\*E-mail: [kwpark@ssu.ac.kr](mailto:kwpark@ssu.ac.kr)

Received: 9 May 2013 / Accepted: 7 June 2013 / Published: 1 July 2013

---

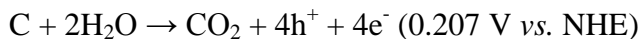
Titanium suboxides (TSO) are generally used in electrochemical devices due to excellent electronic conductivity and enhanced electrochemical stability. We synthesized TSO as a support material through catalytic reaction in the presence of Co catalysts at 800 °C in H<sub>2</sub> atmosphere. The Pt/TSO catalyst shows enhanced electrochemical activity and stability in oxygen reduction reaction in comparison with Pt/C.

---

**Keywords:** Titanium suboxide, Catalytic reaction, Oxygen reduction reaction, Activity, Stability

### 1. INTRODUCTION

Polymer electrolyte membrane fuel cells (PEMFCs) have been of considerable interest because of a variety of merits such as low operating temperatures, high energy density, and applications to automobile industries. In the PEMFCs [1-5], carbon supports are well known as the most effective electrode supports for the hydrogen oxidation and oxygen reduction reaction due to it has higher surface area, excellent electronic conductivity, and, low cost of production [6-8]. In the case of cathode reaction, however, carbon support materials exhibit corrosion of carbon resulting in serious agglomeration of catalysts during electrochemical reaction such as oxygen reduction reaction [9,10]. Furthermore, the carbon corrosion situation is most intensifying during fuel cell start up and shut down, as indicated by the following reaction [11,12]:



Also, the carbon corrosion situation leads to reduce active site of catalysts for agglomeration, coalescence, and dissolution of metallic catalysts.

Accordingly, it has been suggested that the utilization of transition metal oxides as a support is an effective way to promote the electrocatalytic activity and stability for electrochemical reactions. In particular, the transition metal oxides such as  $\text{TiO}_2$ ,  $\text{WO}_3$ ,  $\text{SnO}_2$ ,  $\text{RuO}_2$ ,  $\text{MoO}_3$ , and  $\text{Ta}_2\text{O}_5$  have been reported as alternatives to carbon supports to enhance the catalytic activity and stability for electrochemical reaction [13-18]. However, the transition metal oxide supports for electrochemical reactions have a critical problem such as low electrical conductivity in comparison with carbon materials. The poor electrical conductivity of the supporting material can reduce the electrochemical performance in PEMFCs [19-21].

Recently, it has been reported that the transition metal suboxides as a support material in fuel cells show improved electrochemical stability and electrical conductivity [22]. The typical transition metal suboxides are  $\text{W}_x\text{O}_{3x-1}$ ,  $\text{Mo}_x\text{O}_{3x-1}$ , and  $\text{Ti}_x\text{O}_{2x-1}$ , ( $x = 2, 3, 4, \dots, n$ ) [23,24]. Among them, the titanium suboxides are generally used in various applications such as sensors, photochemical devices, and electrochemical devices due to excellent electronic conductivity, enhanced chemical stability, and commercial availability [25,26]. Wills *et al.* reported that the  $\text{Ti}_x\text{O}_{2x-1}$  ( $x = \text{low value}$ ) have higher conductivity in comparison with other titanium suboxides ( $x = \text{high value}$ ) [27]. However, the transition metal suboxides have been expensive in production due to high reaction temperature ( $T > 1200^\circ\text{C}$ ) or pressure [28,29].

Here, we easily synthesized titanium suboxides (denoted as TSO) as a support material through catalytic reaction at a relatively low temperature. The titanium suboxides were synthesized through catalytic reaction in the presence of cobalt metallic catalyst at 400, 700, and 800  $^\circ\text{C}$  for 3 h in  $\text{H}_2$  atmosphere (Supporting Information). Also, to confirm formation mechanism of titanium suboxide, we synthesized the sample by heat treatment in the presence of the catalyst at 800  $^\circ\text{C}$  for 3 h in  $\text{N}_2$  atmosphere. The structure properties of the NPs were characterized by field-emission transmission electron microscopy (FE-TEM) and X-ray diffraction (XRD). The electrochemical properties of the catalysts were measured and compared using a potentiostat.

## 2. EXPERIMENTAL PART

### 2.1. Synthesis of titanium suboxide using catalytic reaction

The titanium suboxide were prepared using  $\text{TiO}_2$  (Degussa, P-25) as a starting material by means of heat treatment under hydrogen gas atmosphere. For absorption of Co ions as catalyst on  $\text{TiO}_2$  nanoparticles (NPs), the  $\text{TiO}_2$  powder (2 g) and  $\text{CoCl}_6 \cdot 6\text{H}_2\text{O}$  (0.2 g, Aldrich, 98%) were dispersed into 100 ml ethanol (Samchun Chem. Co., 99.9%). The mixed solution was stirred at room temperature for 2 hr and evaporated at 65  $^\circ\text{C}$  and then the obtained powder was dried at 50  $^\circ\text{C}$  oven for 12 h. The as-prepared Co ions deposited on  $\text{TiO}_2$  powders (0.1 g) were put into a quartz boat, and then the quartz boat was set at the quartz tube system under the flow of hydrogen gas. At first, the flow rate of  $\text{N}_2$  gas

was kept for 30 min to get rid of O<sub>2</sub> inside the tube. Under H<sub>2</sub> flow rate of 100 ml min<sup>-1</sup>, the furnace was heated at 400, 700, and 800 °C and then maintained for 3 h. After the heat treatment, the furnace was cooled down to room. Finally, the flow rate of N<sub>2</sub> gas was kept for 30 min to get rid of H<sub>2</sub> inside the tube at room temperature. For investigation of catalyst effect on synthesis of titanium suboxides, in the present synthesis process, we prepared the titanium suboxide NPs in the absence of Co ions using heating treatment in H<sub>2</sub> gas atmosphere at 800 °C. Also, we prepared the titanium suboxide NPs in the presence of Co ions using heating treatment in N<sub>2</sub> gas atmosphere at 800 °C.

### 2.2 Preparation of Pt nanoparticles deposited on titanium suboxides

To prepare supported Pt (20 wt.%) catalysts, 780 mg of titanium suboxide synthesized by heating treatment in H<sub>2</sub> gas atmosphere at 800 °C were dispersed into de-ionized water and then H<sub>2</sub>PtCl<sub>6</sub>•H<sub>2</sub>O (40.9 mg, Aldrich) was dissolved in the solutions with continuous stirring for 1 h. After the stirring, an excess of NaBH<sub>4</sub> (0.20 g, Aldrich) solution as a reductant was added to the mixture solution with continuous stirring at 25 °C for 2 h. The resulting precipitate was washed with de-ionized water several times and dried at 80 °C oven for over night.

### 2.3. Structural analysis

For the structure analysis of the catalysts, X-ray diffraction (XRD) analysis was carried out using a Rigaku X-ray diffractometer with Cu K<sub>α</sub> (λ = 0.15418 nm) source with a Ni filter. The source was operated at 40 kV and 100 mA. The 2θ angular scan from 20° to 60° was explored at a scan rate of 3° min<sup>-1</sup>. For all the XRD measurement, the resolution in the scans was kept at 0.02°. The morphology and size distribution of the catalysts were characterized by field-emission transmission electron microscopy (TEM) using a Tecnai G2 F30 system operating at 300 kV. TEM samples were prepared by placing drops of catalyst suspension dispersed in ethanol on a carbon-coated copper grid. For measurement of the electrical conductivity, the pellets were made by conventional method. The electrical resistance of the compressed pellets was measured in current vs. voltage curves using potentiostat (CH Instrument, CHI 700C) at ambient temperature. Also, the conductivity was calculated by the follow equation:

$$\sigma = \frac{1}{\rho} = \frac{l}{RA}$$

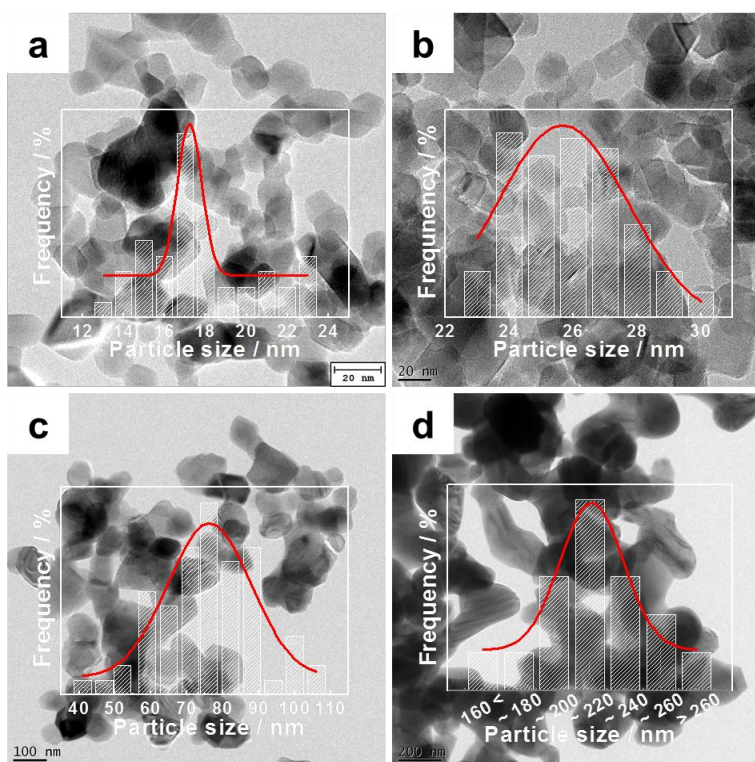
where  $\sigma$  is electrical conductivity (Siemens, S cm<sup>-1</sup>),  $\rho$  is specific resistance,  $l$  is thickness of pellet,  $R$  is resistance, and  $A$  is area of pellet.

### 2.4 Electrochemical analysis

Electrochemical properties of the catalysts were measured in a three-electrode cell at 25 °C using a potentiostat. A Pt wire and Ag/AgCl (in saturated KCl) were used as a counter and reference electrode, respectively. The catalyst ink was prepared by mixing 2 mg metal of all catalysts, 50 μL of

Millipore water, 57.2  $\mu\text{L}$  of 5 wt% Nafion<sup>®</sup> solution (Aldrich), and 195  $\mu\text{L}$  of 2-propanol solution ( $\text{C}_3\text{H}_8\text{O}$ , Sigma). The catalyst ink was dropped onto a glassy carbon working electrode (area  $\sim 0.125664 \text{ cm}^2$ ). After drying in 50  $^\circ\text{C}$  oven, total loading of catalyst was  $47.4 \mu\text{g cm}^{-2}$ . To evaluate electrocatalytic activities of the as-prepared catalysts, CVs were obtained between -0.2 to +1.0 V in Ar-saturated 0.1 M  $\text{HClO}_4$  with a scan rate of  $50 \text{ mV s}^{-1}$  at 25  $^\circ\text{C}$ . The oxygen reduction current–potential curves were obtained using linear sweep voltammetry at various rotation speeds of 1600 rpm in  $\text{O}_2$ -saturated 0.1 M  $\text{HClO}_4$  solution by sweeping the potential from 0.8 to 0 V at a scan rate of  $5 \text{ mV s}^{-1}$ . The accelerated stability test was performed by applying the positive potential of 1.2 V for 30 min in  $\text{O}_2$ -saturated 0.1 M  $\text{HClO}_4$  at 25  $^\circ\text{C}$ .

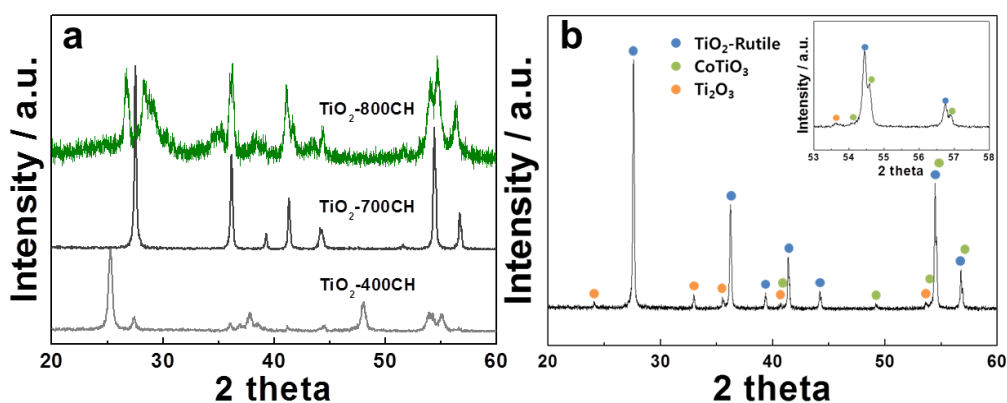
### 3. RESULTS AND DISCUSSION



**Figure 1.** TEM images and size distribution of (a) fresh  $\text{TiO}_2$  (Degussa, Co.), (b)  $\text{TiO}_2$ -400CH, (c)  $\text{TiO}_2$ -700CH, and (d)  $\text{TiO}_2$ -800CH NPs.

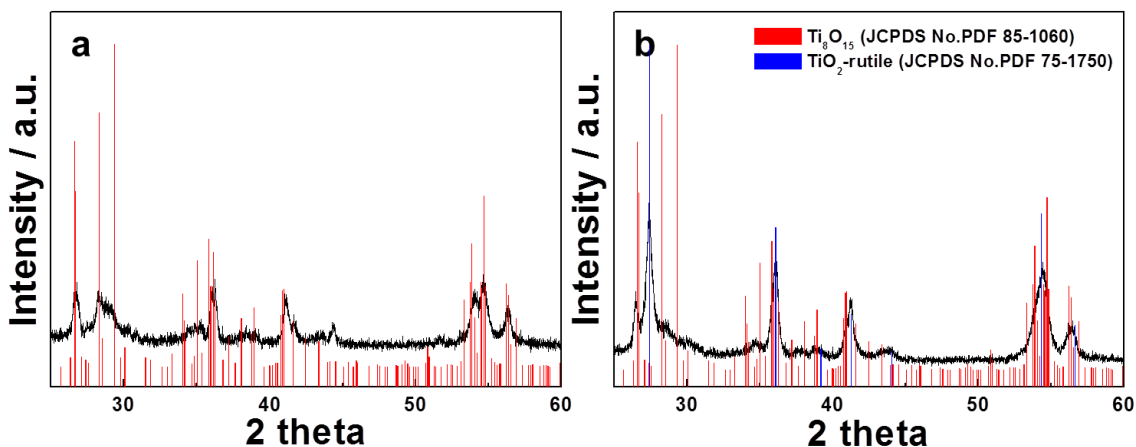
The structural analysis of fresh  $\text{TiO}_2$  (Degussa, Co.) and as-synthesized titanium oxide NPs after heat treatment was carried out by FE-TEM. The fresh  $\text{TiO}_2$  NPs exhibit fairly uniform average particle size of  $17.22 \pm 0.6 \text{ nm}$  as indicated in Fig. 1(a). Fig. 1(b-d) shows FE-TEM images of as-synthesized titanium oxides through catalytic reaction using the catalysts at 400, 700, and 800  $^\circ\text{C}$  in  $\text{H}_2$  atmosphere, respectively (denoted as  $\text{TiO}_2$ -400CH,  $\text{TiO}_2$ -700CH, and  $\text{TiO}_2$ -800CH). The average particle sizes of  $\text{TiO}_2$ -400CH,  $\text{TiO}_2$ -700CH, and  $\text{TiO}_2$ -800CH are  $25.7 \pm 2.1$ ,  $76 \pm 12$ , and  $221 \pm 17$

nm, respectively. As reaction temperature increases, the average particle size of the titanium oxide NPs increases with particle aggregation.



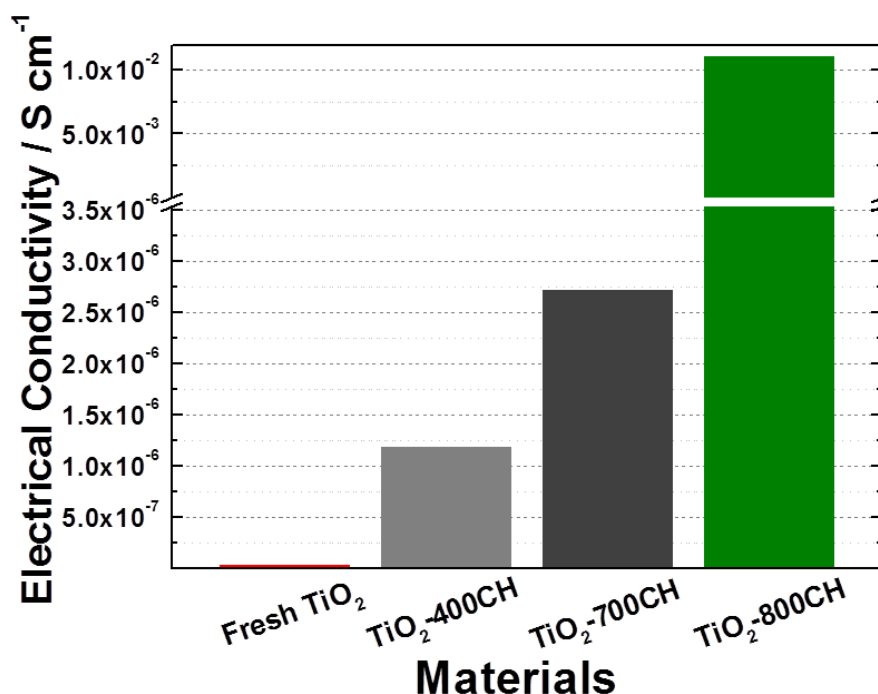
**Figure 2.** (a) XRD patterns of the  $\text{TiO}_2$ -400CH,  $\text{TiO}_2$ -700CH, and  $\text{TiO}_2$ -800CH. (b) XRD pattern of  $\text{TiO}_2$ -800CN [The inset indicates XRD patterns between  $53^\circ$  and  $58^\circ$ ].

Fig. 2(a) shows XRD patterns of as-synthesized titanium oxide NPs through catalytic reaction in the presence of cobalt catalysts under  $\text{H}_2$  atmosphere. The  $\text{TiO}_2$ -400CH and  $\text{TiO}_2$ -700CH exhibit mixed anatase-rutile and homogenous rutile phase, respectively. In contrast, the  $\text{TiO}_2$ -800CH display titanium suboxide phase ( $\text{Ti}_8\text{O}_{15}$ ) (JCPDS No.PDF 85-1060) without typical  $\text{TiO}_2$  phase, i.e. anatase and rutile. Usually, the reduced titanium oxides have been synthesized at considerably high temperatures ( $T > 1200^\circ\text{C}$ ) in  $\text{H}_2$  atmosphere. Herein, it is found that the titanium suboxide can be easily synthesized by catalytic reaction at relatively low-temperature of  $800^\circ\text{C}$ . To understand the formation mechanism of the titanium suboxide using catalytic reaction, we prepared titanium oxide through the catalytic reaction at  $800^\circ\text{C}$  in the presence of Co catalyst under  $\text{N}_2$  atmosphere (denoted as  $\text{TiO}_2$ -800CN). As shown in Fig. 2(b), the XRD pattern of the  $\text{TiO}_2$ -800CN consists of rutile  $\text{TiO}_2$ ,  $\text{CoTiO}_3$ , and  $\text{Ti}_2\text{O}_3$  phase. Among them, the formation of  $\text{CoTiO}_3$  and  $\text{Ti}_2\text{O}_3$  result from cobalt catalysts in the catalytic reaction and oxygen deficiency of  $\text{TiO}_2$  structures, respectively.



**Figure 3.** The XRD patterns of (a)  $\text{TiO}_2$ -800CH and (b)  $\text{TiO}_2$ -800H.

Furthermore, to confirm the effect of metallic cobalt catalyst in the catalytic reaction, we synthesized titanium oxide by prepared at 800 °C in the absence of cobalt catalyst in H<sub>2</sub> atmosphere (denoted as TiO<sub>2</sub>-800H). As indicated in Fig. 3(a), the TiO<sub>2</sub>-800H shows dominant rutile TiO<sub>2</sub> with titanium suboxide (Ti<sub>8</sub>O<sub>15</sub>). Thus, it is concluded that the present synthetic process for titanium suboxides using the catalytic reaction in the presence of Co catalyst under H<sub>2</sub> atmosphere can be a facile method for synthesis of titanium suboxides at relatively low temperature of 800 °C.



**Figure 4.** Electrical conductivity of the fresh TiO<sub>2</sub> (Degussa, Co.), TiO<sub>2</sub>-400CH, TiO<sub>2</sub>-700CH, and TiO<sub>2</sub>-800CH NPs.

Fig. 4 shows electrical conductivity of the as-synthesized titanium oxide NPs through catalytic reaction in the presence of cobalt catalysts under hydrogen atmosphere. The fresh titanium dioxide used as a starting material appears extremely low electrical conductivity ( $2.89 \times 10^{-8} \text{ S cm}^{-1}$ ). The electrical conductivities of the TiO<sub>2</sub>-400CH and TiO<sub>2</sub>-700CH are  $1.18 \times 10^{-6}$  and  $2.76 \times 10^{-6} \text{ S cm}^{-1}$ , respectively. On the other hand, the TiO<sub>2</sub>-800CH exhibits  $\sim 10^4$  times higher electrical conductivity ( $1.10 \times 10^{-2} \text{ S cm}^{-1}$ ) in comparison with other titanium oxides. For electrochemical analysis, we prepared Pt NPs deposited on the TiO<sub>2</sub>-800CH (denoted as Pt/TSO) having the highest electrical conductivity and suboxide structure. To identify electrochemical properties of the catalyst, as shown in Fig. 5(a), cyclic voltammograms (CVs) were obtained in Ar-saturated 0.1 M HClO<sub>4</sub> between -0.2 and +1.0 V (vs. Ag/AgCl). The ORR activity of the Pt/TSO was measured using linear sweep voltammetry (LSV) in O<sub>2</sub>-saturated HClO<sub>4</sub> solution between 0.0 and +0.8 V in comparison with typical Pt/C in Fig. 5(c and d). The Pt/TSO exhibits an improved oxygen reduction activity in comparison with the Pt/C. At 0.55 V as half-wave potential [30,31], the current density ( $3.07 \text{ mA cm}^{-2}$ ) of the Pt/TSO for ORR is 1.60 times higher than that of the Pt/C ( $1.92 \text{ mA cm}^{-2}$ ). The ORR activities of the Pt/TSO and Pt/C

before and after the accelerated stability test were measured by comparing current density of the LSVs at 0.55 V as shown in Fig. 5(c and d). The ORR accelerated stability test was performed by applying the positive potential of 1.4 V (*vs.* NHE) for 30 min in O<sub>2</sub>-saturated 0.1 M HClO<sub>4</sub> at 25 °C [32-34]. In Fig. 5(c), the Pt/TSO exhibits a negligible loss in ORR activity after the accelerated stability test.

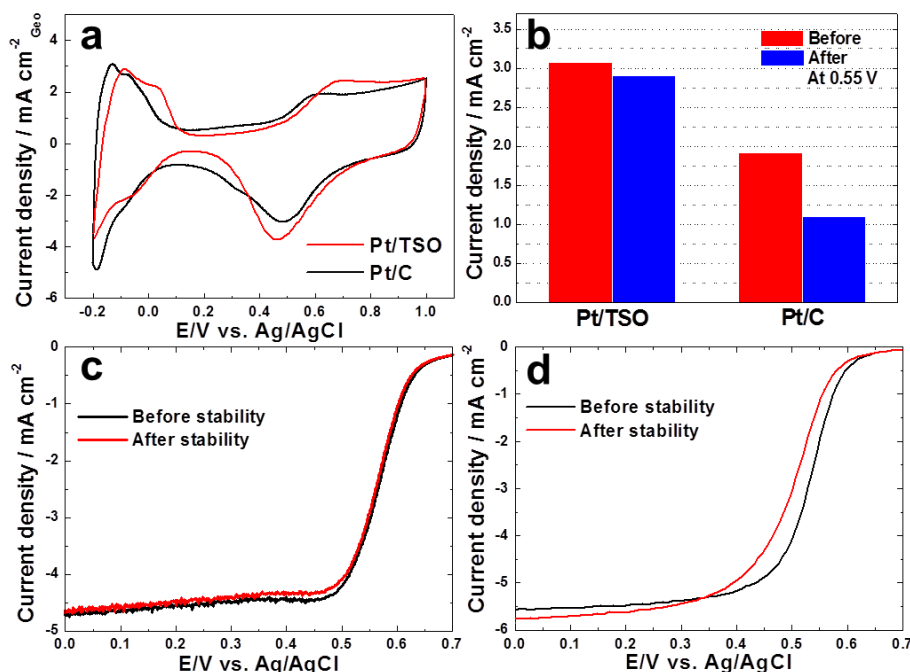


**Figure 5.** (a) CVs of Pt/TSO and Pt/C in Ar-saturated 0.1 M HClO<sub>4</sub>. (b) Comparison of ORR current density at 0.55 V of Pt/TSO and Pt/C before and after the accelerated stability test in Figure 4c and d. ORR polarization curves of (c) Pt/TSO and (d) Pt/C before and after the accelerated stability test in O<sub>2</sub>-saturated 0.1 M HClO<sub>4</sub>.

In contrast, the Pt/C exhibits a considerable loss in ORR activity between +0.4 and +0.6 V, representing an activation polarization loss of the catalysts as indicated in Fig. 6(d). Furthermore, based on the geometric area of the glassy carbon electrode, the current density of the Pt/TSO at 0.55 V after the accelerated stability test is slight loss of 5.21 % whereas the Pt/C exhibits serious loss of 42.7% as indicated in Fig. 5(b). Krishnan *et al.* reported that the titanium suboxides as corrosion-resistant supports exhibit improved stability in oxygen reduction reaction [35]. Thus, we can demonstrate that the Pt/TSO displays enhanced electrocatalytic properties due to highly improved electrical conductivity and stability.

#### 4. CONCLUSIONS

In summary, we synthesized electrical conductive titanium suboxides as a support material through catalytic reaction process in the presence of catalysts at relatively low-temperature. The as-

synthesized titanium suboxide support exhibited highly improved electrical conductivity. For the oxygen reduction reaction, the Pt/TSO showed much improved electrochemical activity and stability.

#### ACKNOWLEDGMENTS

This work was supported by the Ministry of Knowledge Economy(MKE) and Korea Industrial Technology Foundation (KOTEF) through the Human Resource Training Project for Strategic Technology and New & Renewable Energy R&D Program (2011301003007A) of the Ministry of Knowledge and Economy.

#### References

1. H. Zhang and P. K. Shen, *Chem. Rev.*, 8 (2012) 2780.
2. S.-W. Xie, S. Chen, Z.-Q. Liu and C.-W. Xu, *Int. J. Electrochem. Sci.*, 6 (2011) 882.
3. S.-J. Kim, Y.-W. Lee, S.-B. Han, S.-B. Kim, W.-S. Kim and K.-W. Park, *Int. J. Electrochem. Sci.*, 8 (2013) 3825.
4. Y.-W. Lee, A.-R. Ko, D.-Y. Kim, S.-B. Han and K.-Y. Park, *RSC Adv.*, 2 (2012) 1119.
5. J. M. S. Ayub, R. F. B. De Souza, J. C. M. Silva, R. M. Piasentin, E. V. Spinacé, M. C. Santos and A. O. Neto, *Int. J. Electrochem. Sci.*, 7 (2012) 11351.
6. S. M. Lyth, Y. Nabae, S. Moriya, S. Kuroki, M.-A. Kakimoto, J.-I. Ozaki and S. Miyata, *J. Phys. Chem. C*, 113 (2009) 20148.
7. J.-S. Zheng, X.-Z. Wang, R. Fu, P. Li, D.-J. Yang, H. Lu and J.-X. Ma, *New Carbon Mater.*, 26 (2011) 262.
8. H.-W. Oh, J.-G. Oh, W. H. Lee, H.-J. Kim and H. Kim, *Int. J. Hydrogen Energy*, 36 (2011) 8181.
9. S. G. Chalk and J. F. Miller, *J. Power Sources*, 159 (2006) 73.
10. M. S. Wilson, J. H. Garzon, K. E. Sickafus and S. Gottesfeld, *J. Electrochem. Soc.*, 140 (1993) 2872.
11. K. Kinoshita, *Carbon: Electrochemical and Physico-chemical Properties*, Wiley, New York, (1988).
12. S.-Y. Huang, P. Ganesan, S. Park and B. N. Popov, *J. Am. Chem. Soc.*, 131 (2009) 13898.
13. K. Drew, G. Girishkumar, K. Vinodgopal and P. V. Kamat, *J. Phys. Chem. B*, 109 (2005) 11851.
14. J.-M. Lee, S.-B. Han, Y.-W. Lee, Y.-J. Song, J.-Y. Kim and K.-W. Park, *J. Alloy. Compd.*, 506 (2010) 57.
15. A.-R. Ko, J.-Y. Kim, J.-K. Oh, H.-S. Kim, Y.-W. Lee, S.-B. Han and K.-W. Park, *Phys. Chem. Chem. Phys.*, 12 (2010) 15181.
16. J.-K. Shin, S. M. Jeong, Y. Tak and S.-H. Baeck, *Res. Chem. Intermed.*, 36 (2010) 715.
17. C. Zhou, H. Wang, P. Peng, J. Liang, H. Yu and J. Yang, *Langmuir*, 25 (2009) 7711.
18. K.-W. Park, Y.-E. Sung and M. F. Toney, *Electrochem. Commun.*, 7 (2005) 151.
19. S. Yoon, C. Jo, S. Y. Noh, C. W. Lee, J. H. Song and J. Lee, *Phys. Chem. Chem. Phys.*, 13 (2011) 11060.
20. F. Jiao, K. M. Shaju and P. G. Bruce, *Angew. Chem. Int. Ed.*, 44 (2005) 6550.
21. J. Lee, M. C. Orilall, S. C. Warren, M. Kamperman, F. J. DiSalvo and U. Wiesner, *Nat. Mater.*, 7 (2008) 222.
22. Y. Ye, J. Joo, B. Lim and J. Lee, *Chem. Eur. J.*, 18 (2012) 2797.
23. S. Shi, X. Xue, P. Feng, Y. Liu, H. Zhao and T. Wang, *J. Cryst. Growth*, 310 (2008) 462.
24. S. Yoon, E. Kang, J. K. Kim, C. W. Lee and J. Lee, *Chem. Commun.*, 47 (2011) 1021.
25. A. Kitada, G. Hasegawa, Y. Kobayashi, K. Kanamori, K. Nakanishi and H. Kageyama, *J. Am. Chem. Soc.*, 134 (2012) 10894.
26. S.-I. Ohkoshi, Y. Tsunobuchi, T. Matsuda, K. Hashimoto, A. Namai, F. Hakoe and H. Tokoro, *Nat. Chem.*, 2 (2010) 539.
27. F. C. Walsh and G. R. Wills, *Electrochim. Acta*, 55 (2010) 6342.

28. S.-Y. Park, S.-I. Mho, E. O. Chi, Y. U. Kwon and H. L. Park, *Thin Solid Films*, 258 (1995) 5.
29. C. Tang, D. Zhou and Q. Zhang, *Mater. Lett.*, 79 (2012) 42.
30. J. Zhang, K. Sasaki, E. Sutter and R. R. Adzic, *Science*, 315 (2007) 220.
31. M.-H. Shao, K. Sasaki and R. R. Adzic, *J. Am. Chem. Soc.*, 128 (2006) 3526.
32. H. S. Oh, J. G. Oh, S. Haam, K. Arunabha, B. Roh, I. Hwang and H. Kim, *Electrochem. Commun.*, 10 (2008) 1048.
33. S.-E. Jang and H. Kim, *J. Am. Chem. Soc.*, 132 (2010) 14700.
34. Y.-J. Ko, H.-S. Oh and H.-S. Kim, *J. Power Sources*, 195 (2010) 2623.
35. P. Krishnan, S. G. Advani and A. K. Prasad, *J. Solid State Electrochem.*, 16 (2012) 2515.